

Frascati Physics Series Vol. XLVI (2007), pp. 000-000

/

H ADRON07: XII Int. Conf. on Hadron Spectroscopy – Frascati, October 8-13, 2007

Parallel Session

LIGHT HADRON SPECTRUM IN THE INSTANTON LIQUID MODEL

P. Faccioli

Dipartimento di Fisica, Università degli Studi di Trento and I.N.F.N.

M. Cristoforetti,

Physik Department, Technische Universität München

M.C. Tichy,

*Institut für Theoretische Physik, Universität Tübingen,
and Dipartimento di Fisica, Università degli Studi di Trento*

M.Traini,

*and Dipartimento di Fisica, Università degli Studi di Trento, I.N.F.N. and E.C.T.**

Abstract

We review our recent study of the role played by the chiral interactions induced by instantons, in the lowest-lying sector of the light hadron spectrum. We discuss how the ordering of the lowest meson and baryon excitations is explained by the structure of the instanton-induced quark-quark and gluon-gluon interaction. We focus on the pion, nucleon, vector- and axial-vector mesons, and on the scalar glueball. We find that all these hadrons are bound in this model and have realistic masses.

1 Introduction

The spectrum of the lightest hadrons encodes the information about the way the u - and d - quarks interact with gluons, at different distance scales. The ~ 400 MeV splitting between parity partners, e.g. vector- and axial-vector-

mesons, suggests that the interactions associated with the spontaneous breaking of chiral symmetry are very important in the low-lying sector of the spectrum. Similarly, the large splitting between the pion and the η' implies that topological interactions related to the axial anomaly are giving significant contribution. On the other hand, splitting between parity-partners is much reduced for higher resonances, and there have been claims that chiral symmetry may even be restored, up in the spectrum ¹⁾.

At a qualitative level, the large contribution of the chiral forces to the internal dynamics of the lowest-lying hadrons can be explained as follows. The wave-function of the ground-state hadrons and of the lowest resonances is narrower than that of the higher excitations. Consequently, quarks in low-lying states and low-lying resonances are on average closer to each other and therefore relatively less sensitive to the very long-distance, confining part of the quark-quark interaction. On the other hand, they are very sensitive to the non-perturbative correlations which take place at the intermediate distance scales, $\sim 1/\Lambda_\chi \sim 0.2 - 0.3$ fm, where Λ_χ is the scale associated to chiral symmetry breaking. Conversely, up in the spectrum, the hadron wave-function extends for larger distances and quarks begin to experience the effect of the confining forces, which take place at the QCD scale $1/\Lambda_{QCD} \sim 1$ fm.

Within such a scenario, two questions emerge naturally: (i) what is the microscopic origin of the interactions associated with the spontaneous breaking of chiral symmetry? (ii) are any of the light hadrons completely dominated by such chiral forces, to a point that they would exist even if confining correlations were completely removed? In this talk, I will review our recent attempts to address these questions in the context of the Interacting Instanton Liquid Model (IILM).

It has long been argued that instantons of size ~ 0.3 fm represent the main vacuum gauge field configurations responsible for the non-perturbative dynamics at the chiral scale ²⁾. Recent lattice studies ³⁾ have provided strong evidence in support of such an hypothesis. As a consequence of the spontaneous breaking of chiral symmetry, quark propagating in the instanton vacuum develop an effective mass of $\sim 350-400$ MeV, hence this model provides a connection between current and constituent quarks.

The main drawback of the instanton models is that they do not provide confinement. On the one hand, this is a serious problem. It implies that instan-

tons cannot be the only important non-perturbative gauge field fluctuations in the QCD vacuum. On the other hand, just because of the lack of confinement, the instanton models represent a convenient framework in which the effect of chiral symmetry breaking can be isolated and the questions listed above can be addressed.

2 The instanton-induced interaction in the different hadrons

The interaction generated by instantons is not equally important in all hadrons. Due to the specific quantum-number structure of the 't Hooft vertex, and of the instanton gauge field there are channels in which the instanton effect come at leading order in the instanton vacuum diluteness, $\kappa \sim 0.1$ and channels in which they come at sub-leading orders. This feature of the model is very important as it provides a natural explanation to a number of observed phenomena ⁴⁾: for example, it explains the well-known $\Delta I = 1/2$ rule for non-leptonic hyperon and kaon decays, or the very early on-set of the perturbative regime in the $\gamma\gamma^* \rightarrow \pi^0$ transition form factor, relative to the strongly non-perturbative behavior of the space-like pion form factor ⁵⁾.

As far as the hadron spectrum is concerned, the structure of the instanton-induced interaction correctly accounts for the ordering of the lowest-lying states, i.e. where we expect chiral forces to be important. In fact, leading instanton forces are most attractive in the pion, but are suppressed in the ρ -meson and A_1 -meson and are even repulsive in the η' -meson. Similarly, they are very strong and attractive in the nucleon and are suppressed in the Δ -isobar. Remarkably, the same dynamical mechanism can explain also the ordering of the lightest glueball excitations observed in lattice QCD simulations, with strong attraction in the scalar channel, suppression in the tensor channel and repulsion in the pseudo-scalar channel.

3 Hadron Mass Calculation in the IILM

In the IILM, the QCD path integral over all possible gluon field configurations is replaced by

$$\mathcal{Z}_{QCD} \simeq \mathcal{Z}_{ILM} = \sum_{N_+, N_-} \frac{1}{N_+! N_-!} \int \prod_i^{N_+ + N_-} d\Omega_i d(\rho_i) e^{-S_{int}} \prod_i^{N_f} \det(i\mathcal{D} + im_f) \quad (1)$$

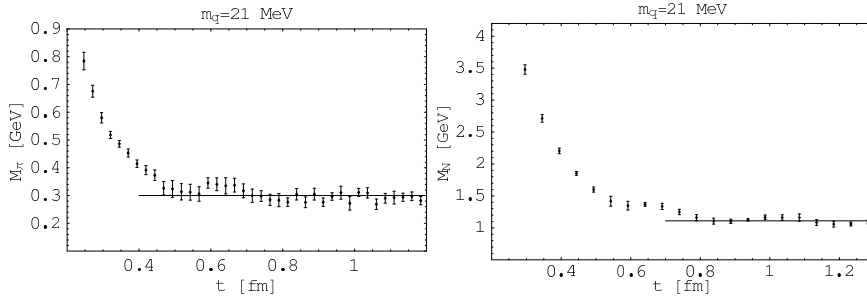


Figure 1: Typical effective mass plots obtained in the IILM and used to extract the pion (left panel) and nucleon (right panel) masses.

Here, $d\Omega_i = dU_i d^4z_i d\rho_i$ is the measure in the space of collective coordinates, color orientation, position and size, associated with the single instantons. Quantum fluctuations are included in Gaussian approximation, through the semi-classical instanton amplitude $d(\rho_i)$. S_{int} is a bosonic interaction between pseudo-particles which includes a long-distance attractive interaction derived semi-classically and a short-range repulsive core, introduced phenomenologically in order to remove large-sized instantons from the vacuum. In the formulation of the model we have considered ⁷⁾, the strength of such a repulsion is the only phenomenological parameter, which has to be tuned to reproduce observations.

In a field-theoretic framework, the information about the hadron spectrum is encoded in the two-point Euclidean correlation functions,

$$G_H(\tau) = \int d^3\underline{x} \langle 0 | T [j_H(\underline{x}, \tau) \bar{j}_H(\underline{0}, 0)] | 0 \rangle, \quad (2)$$

where J_H is an operator which excites states of hadrons with the quantum numbers of the hadron H . Once such a correlation function has been evaluated, the mass of lowest-lying stable hadron can then be extracted from the plateau in the large Euclidean time limit of the effective mass, i.e. using

$$M_H = \lim_{\tau \rightarrow \infty} M_H^{eff}(\tau) \quad M_H^{eff}(\tau) = \frac{1}{\Delta\tau} \ln \frac{G_H(\tau)}{G_H(\tau + \Delta\tau)}. \quad (3)$$

The pion and the nucleon are the two hadrons in which the instanton-induced

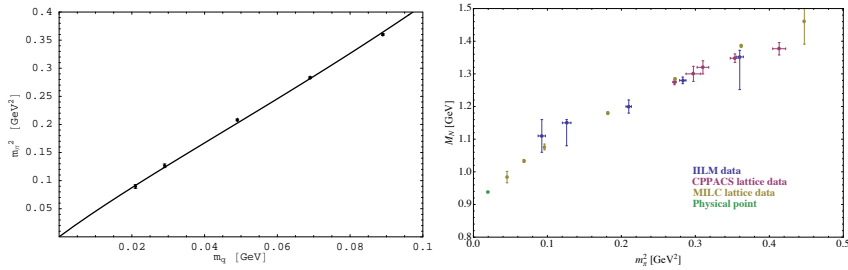


Figure 2: Left Panel: The pion mass as a function of the quark mass obtained in the IILM and compared with the extrapolation formula derived from chiral perturbation theory. Right Panel: The nucleon mass as a function of the pion mass squared obtained in IILM and in lattice calculations.

interaction is most intense. Typical effective mass plots obtained from IILM calculations ⁷⁾ are shown in Fig.1 and are qualitatively indistinguishable from those obtained in lattice QCD simulations. They clearly display a plateau, which is the signature for the existence of a bound-state. We have extracted the hadron masses corresponding to five different values of the quark mass in the range $20 < m_q < 90$ MeV. The behavior of the pion (nucleon) mass with m_q (m_π^2) is presented in Fig. 2. We have fitted the chiral behavior of the pion mass on the quark mass using the extrapolation formula obtained to $\mathcal{O}(p^2)$ from chiral perturbation theory. This leads to low-energy effective coefficients $f_0 = 85$ MeV and $\langle \bar{q}q \rangle = (-259\text{MeV})^3$, in excellent agreement with phenomenology. On the other hand, the calculated nucleon masses at different values of the pion mass agree very well with the available results of lattice QCD simulations.

Extracting information about the mass of the unstable vector and axial-vector meson resonances from the effective mass plot analysis is much harder than in the case of ground-state hadrons. In fact, if the quark mass is sufficiently small, the effective mass does not converge to the mass of the lowest resonance, but to the invariant mass of the decay products, at threshold. In order to be able to extract the masses of ρ and A_1 mesons from IILM correlations functions, the expected specific functional form of their effective mass was

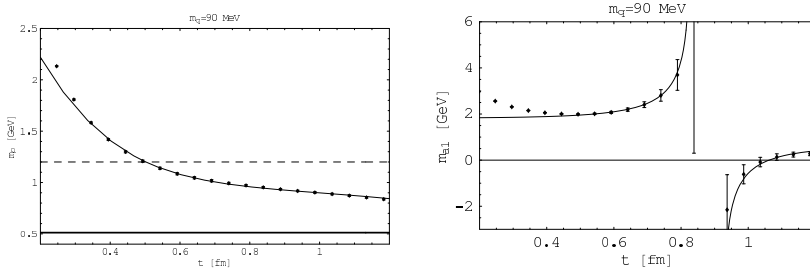


Figure 3: The effective mass plot for the ρ -meson (left panel) and A_1 meson (right panel) evaluated in the IILM (points) and compared with the behavior expected from the structure of the spectral function (line). The significance of the thick line and of the dashed line is explained in the original paper ⁸⁾

investigated in detail in ⁸⁾, by using the experimental information about their spectral function, available from ALEPH. In Fig. 3 we compare the expected shape of the effective mass (line) with the points obtained in the IILM and find agreement. Note that the singularity in the axial-vector channel arises from the interference of the pion and axial-vector contributions and therefore represent a clean evidence that both such states exist in the instanton vacuum.

On the other hand, we have found that the calculated ρ - and A_1 - meson mass are almost 30% larger than the experimental value. This fact can be interpreted as a signature that, in such hadrons, confinement begins to play an significant role.

We conclude this section by mentioning our recent calculation of the mass of the scalar glueball, in the instanton vacuum ⁹⁾. While numerical calculations completely analog to the ones performed for the nucleon and pion are in presently progress, here we discuss our recent results based on the Single Instanton Approximation (SIA) ¹⁰⁾.

The SIA follows from the observation that if the instanton liquid is sufficiently dilute, short-sized correlation functions are saturated by the contribution of a *single* pseudo-particle in the ensemble, the one closest to the endpoints of the correlator.

The main advantage of the SIA is that it allows to obtain predictions from

analytic calculations, rather than from Monte Carlo numerical simulations. The prize to pay is that the SIA can be used to compute correlation functions with external momenta of the order of several GeV and for Euclidean times smaller than ~ 1 fm.

In order to reliably use the SIA, it is convenient to introduce a *momentum-dependent effective mass*,

$$M_{eff}(\tau, \mathbf{p}) = \sqrt{E_{eff}^2(\tau, \mathbf{p}) - \mathbf{p}^2}, \quad E_{eff}(\tau, \mathbf{p}) = -\frac{d}{d\tau} \log G_S(\tau, \mathbf{p}). \quad (4)$$

It is straightforward to show that, if the lowest scalar glueball excitation in the spectrum is a single-particle bound-state, then in the large Euclidean time limit $M_{eff}(\tau, \mathbf{p})$ must stop depending on τ and on \mathbf{p} and converge to the glueball's mass: $\lim_{\tau \rightarrow \infty} M_{eff}(\tau, \mathbf{p}) = M_{0^{++}}$.

Results for the SIA momentum-dependent effective mass $M_{eff}(\tau, \mathbf{p})$ are reported in Fig. 4, which shows how the effective mass plot calculated at two different momenta, in a range of different average instanton sizes. These plots clearly show that there exists a range of Euclidean times for which the momentum-dependent effective mass becomes independent on both momentum and Euclidean time. The scalar glueball mass predicted by the model is $M_{0^{++}} = 1.290 - 1.420$ GeV, in good agreement with the recent results of lattice calculations of Meyer and Teper¹¹⁾ $M_{0^{++}}^{latt.} = 1475(30)_{stat.}(65)_{sys.}$ MeV. At very large times, the SIA breaks down and the correlators start depending on τ again.

4 Conclusions

In this talk, we have reviewed our recent attempts to use the IILM to investigate the structure of the lowest-lying part of the hadron spectrum. We have found that nucleon, pion, vector- and axial- vector mesons as well as the lightest scalar glueball can be bound and have realistic masses, even in the absence of confinement. These results complement previous studies, in which it was shown that also the electro-weak structure of light hadrons can be well understood in this model^{5, 6)}.

References

1. L. Ya. Glozman, [arXiv: hep-ph/0701081]

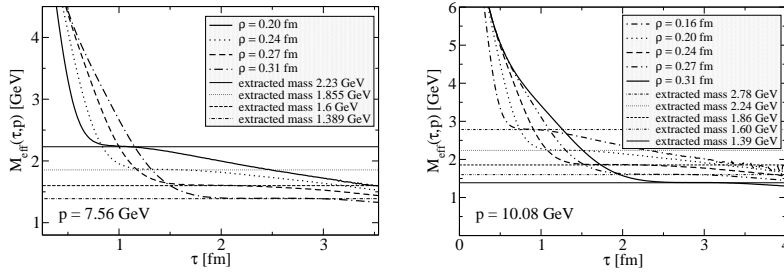


Figure 4: The momentum-dependent effective mass plot for the scalar glueball mass evaluated at for several average instanton sizes and two different momenta.

2. E.V.Shuryak, Nucl. Phys. **B214** (1982), 237. D. Diakonov and V. Petrov: Nucl. Phys. **B245** (1984), 259.
3. C. Gatttringer, Phys. Rev. Lett. **88** (2002), 221601. C. Gatttringer *et al.*, Nucl. Phys. **B617** (2001) 101. P. Faccioli and T. A. De Grand, Phys. Rev. Lett. **91** (2003), 182001.
4. P.Faccioli, Int. J. Mod. Phys. **A20** (2005): 4615.
5. M. Cristoforetti *et al.* Phys. Rev. **D70** (2004) 054016. P. Faccioli, A. Schwenk and E.V. Shuryak, Phys. Rev. **D67** (2003) 113009.
6. P. Faccioli, Phys. Rev. **C69** (2004) 065211. P. Faccioli and E.V. Shuryak, Phys. Rev. **D65** (2002) 076002. P. Faccioli, A. Schwenk and E.V. Shuryak, Phys. Lett. **B549** (2002) 93.
7. M.Cristoforetti, P.Faccioli, J.Negele and M.Traini, Phys. Rev. **D75** (2007), 034008.
8. M.Cristoforetti, P.Faccioli and M.Traini Phys. Rev. **D75** (2007), 054024.
9. C.M.Tichy and P.Faccioli, [arXiv:0711.3829 (hep-ph)]
10. P. Faccioli and E.V. Shuryak, Phys. Rev. **D64** (2002) 114020. P.Faccioli, Phys. Rev. **D65** (2002) 094014.
11. H. B. Meyer and M. J. Teper, Phys. Lett. B **605** (2005), 344